Supporting information

Dynamic contrast enhanced CEST MRI using a low molecular weight dextran

Zheng Han[1,2,†], Chuheng Chen[3,†], Xiang Xu[1,2], Renyuan Bai[4], Verena Staedtke[4], Jianpan Huang[5], Kannie W.Y. Chan[1,5], Jiadi Xu[1,2], David O. Kamson[6], Zhibo Wen[7], Linda Knutsson[1,8], Peter C.M. van Zijl[1,2], and Guanshu Liu[1,2] *

[1] Department of Radiology, Johns Hopkins University, Baltimore, MD, USA

[2] F.M. Kirby Research Center for Functional Brain Imaging, Kennedy Krieger Institute, Baltimore, MD, USA

[3] Department of Biomedical Engineering, Case Western Reserve University, Cleveland, USA

[4] Department of Neurology and Neurosurgery, Johns Hopkins University, Baltimore, MD, USA

[5] Department of Biomedical Engineering, City University of Hong Kong, Hong Kong, China.

[6] The Sidney Kimmel Comprehensive Cancer Center at Johns Hopkins University, Baltimore, MD, USA.

[7] Department of Radiology, Zhujiang Hospital, Southern Medical University, Guangzhou, Guangdong, China

[8] Department of Medical Radiation Physics, Lund University, Lund, Sweden

[†]: These authors contributed equally to this work

* Corresponding author:

Guanshu Liu, Ph.D.

707 N. Broadway, Baltimore, MD 21205

Phone (office): 443-923-9500; Fax: 410-614-3147

Email: guanshu@mri.jhu.edu

Supplementary Methods

S1. Estimation of exchange rate k_{ex} using T_2 relaxation times

The exchange rate was estimated using the classic Swift-Connick equation (Eq S1) according to our previously published protocol (1-3). In brief, the Swift-Connick equation describes the relationship between the chemical shift difference of the exchangeable proton with respect to water resonance ($\Delta\omega$ =1.2 ppm for Dex1 in the present study), exchange rate (k_{ex}, to be determined), and R_{2ex} is the measured T_2 relaxation rate in the presence of exchange (R_{2ex}= $1/T_{2ex}$), which were measured using the CPMG sequences as described below.
Of note, the unit of $\Delta\omega$ is rad/s (4,5).

$$R_{2\mathrm{ex}} = k_{\mathrm{ex}} P_{\mathrm{B}} \frac{\Delta\omega^2}{k_{\mathrm{ex}}^2 + \Delta\omega^2} \qquad \text{Eq. S1}$$

P_B is the fraction of exchangeable protons. Using an average of 3 OH groups per glucose unit (6) and 6 glucose units in each Dex1 and 110 M protons in water, PB equals 1.63 x 10^{-5} per mM glucose unit.

$$r_{2ex} = (1.63 \times 10^{-5}) \frac{k_{ex} \cdot \Delta\omega^2}{{k_{ex}}^2 + \Delta\omega^2} \qquad \text{Eq. S2}$$

R_2 relaxation rates were acquired using a Carr-Purcell-Meiboom-Gill (CPMG) method.(3) Briefly, a T_2 preparation module was added in the front of a fast spin-echo imaging readout, i.e., Rapid Acquisition with Relaxation Enhancement (RARE) pulse sequence. The T_2 preparation period consisted of different numbers of CPMG segments with the inter-echo time t_{CPMG} fixed at 10 ms. A total of 16 CPMG-weighted images were acquired with the number of segments varied from 2 to 1024, corresponding to echo times of 20 ms - 10.24 sec. The imaging parameters were: TR/TE = 25000/4.3 ms, RARE factor = 16, a 64x64 acquisition matrix with a spatial resolution of *c.a.* 250x250 μm^2, and slice thickness of 1 mm. The acquisition time for each T_2-weighted image was 1 min 40 s. To obtain the exchange-based relaxivity rate, r_{2ex} , of each compound, the R_2=1/T_2 water proton relaxation rates of the compound solutions at different concentrations, i.e., 1, 2, 5 and 10 mM, were measured and fitted to Equation S3.

$$R_2 = R_2^0 + r_{2ex} \times [C] \qquad \text{Eq. S3}$$

Where R_2^0 is the inherent water proton R_2 transverse relaxation rate of the solvent and [C] is the concentration of the agent.

It should be noted that, with a single measured r_{2ex}, two k_{ex} values are obtained when solving the Swift-Connick equation. Because it is well known that hydroxyl protons are fast-exchanging at physiological pH and temperature, the fast k_{ex} was chosen.

Supplementary Results

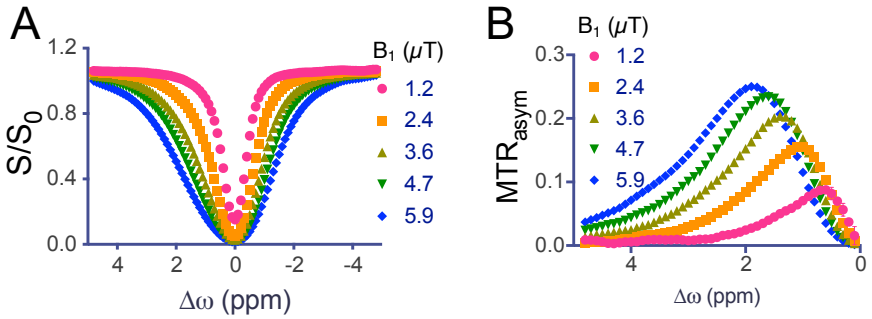

Figure S1. B_1 dependence of the CEST MRI signal of 20 mM Dex1 at 11.7T. **A**) Z-spectra; **B**) MTR_{asym} plots. B_1 is in μT. Note that the peak values shift with respect to B_1 due to the effect of direct water saturation.

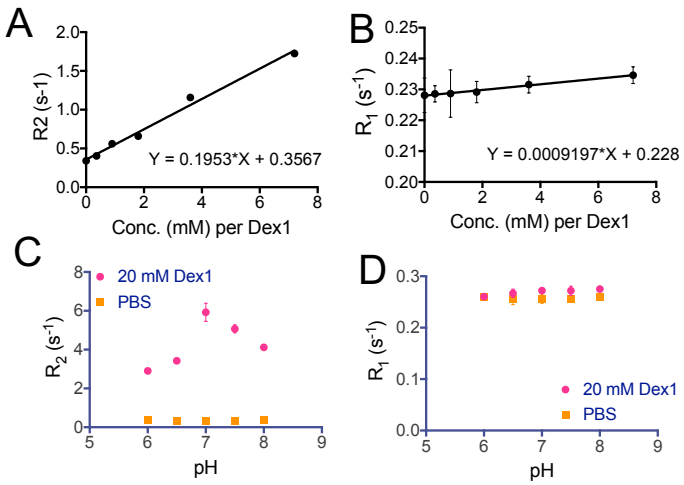

Figure S2. The T_1 and T_2 contrast-enhancing ability of Dex1 at 11.7T. A) $R_2 = 1/T_2$ and **B**) $R_1 = 1/T_1$ of Dex1 at different concentrations. **C)** R_2 and **D**) R_1 of 20 mM Dex1 and PBS (control) as a function of pH.

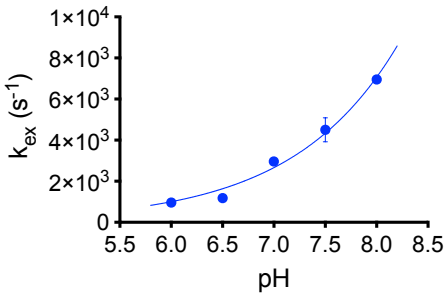

Figure S3. Exchange rate of OH protons in Dex1 as the function of pH at 37 °C in PBS. The exchange rate of hydroxyl proton at each pH was estimated using the measured R_2 relaxation time as described above.

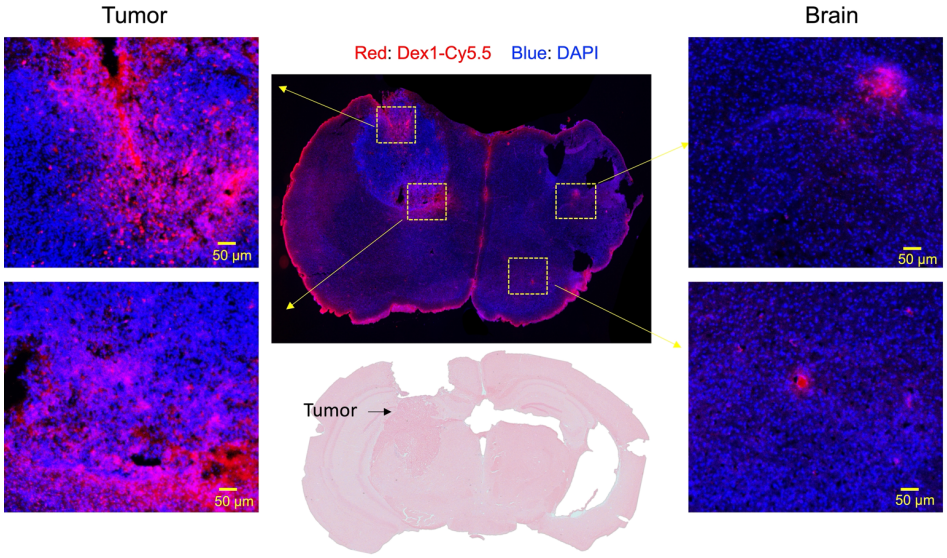

Figure S4. Immunofluorescence images showing the distribution of Dex1 in a representative tumor-bearing mouse brain. On the images, blue indicates nuclei (stained with DAPI), whereas red indicates Dex1 (labeled with Cy5.5). Four zoomed views of different tumor and brain regions are shown on the left and right panels, respectively. Shown below is a H&E-stained image as the reference.

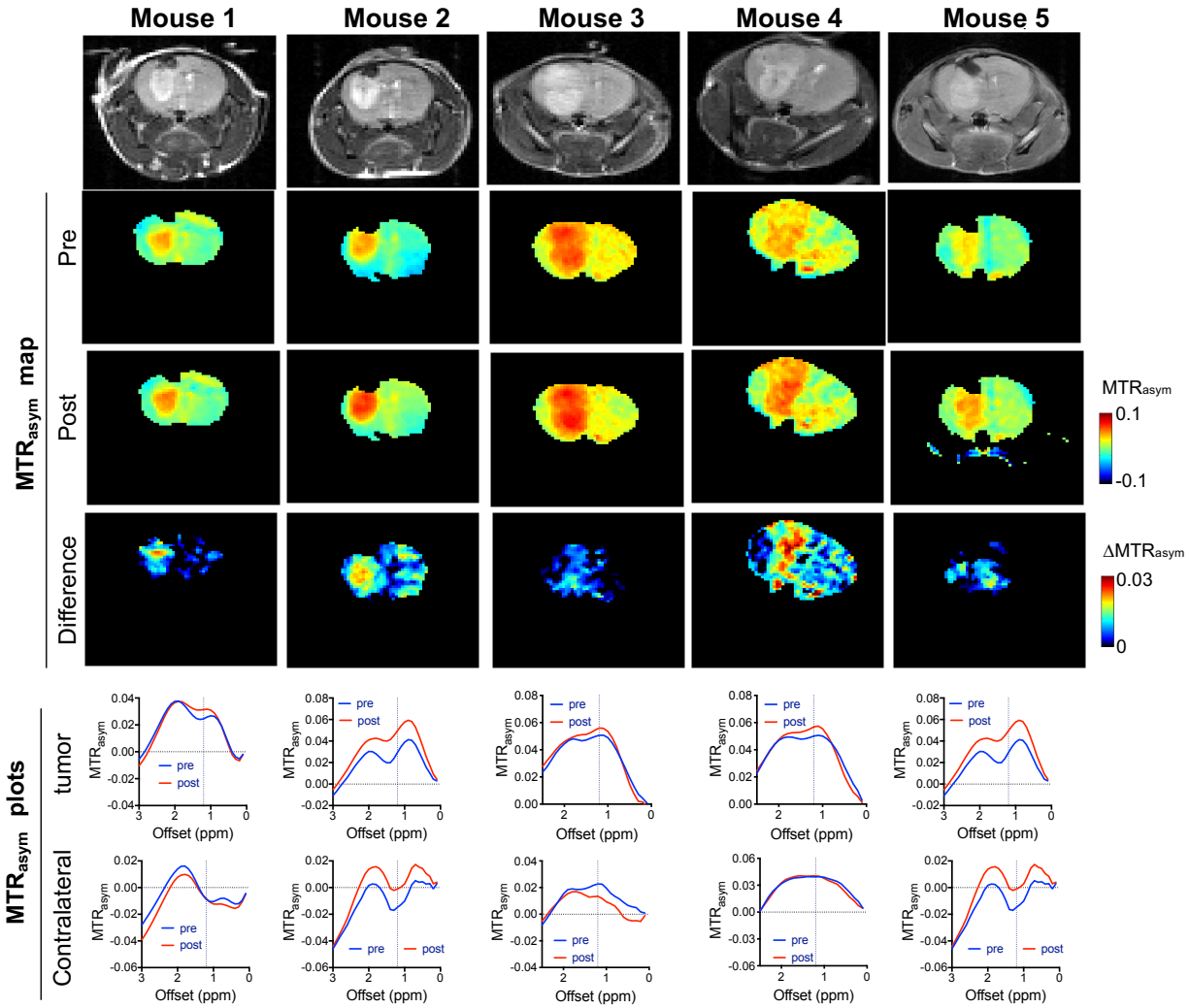

Figure S5. Dex1-enhanced CEST MRI at 11.7T in all five mice.

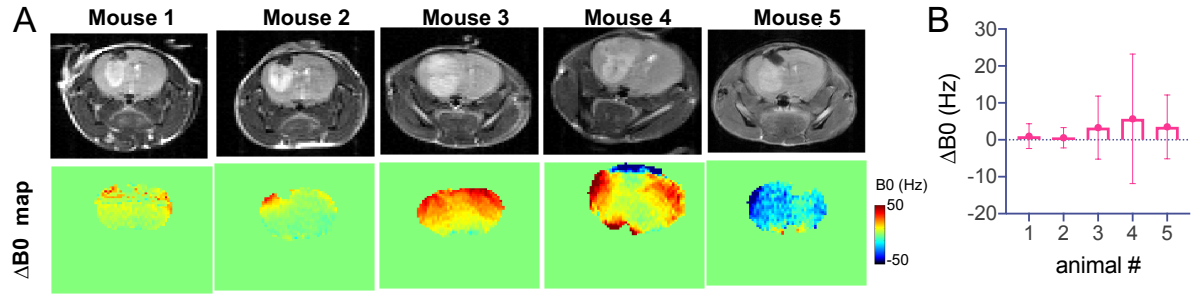

Figure S6. Assessment of the changes in B_0 inhomogeneity after Dex1 infusion at 11.7T.

A) ΔB0 maps of all five animals. B) Bar plots showing the means and standard deviations of the whole brain region of each animal.

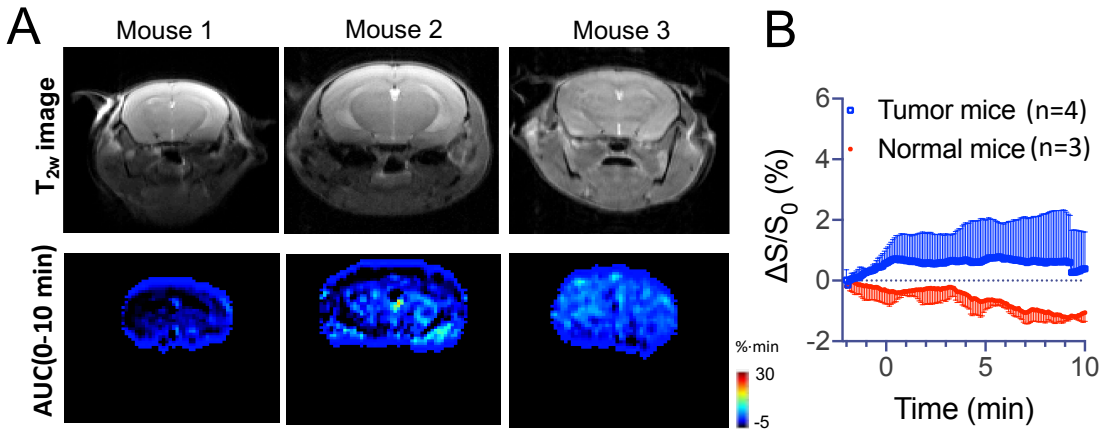

Figure S7. DDE CEST MRI in the normal mouse brain at 11.7T. **A**) T2w and corresponding AUC(0-10 min) maps of all three non-tumor-bearing normal mice studied. **B**) Mean dynamic CEST signal change in the brain ROIs in either non-tumor-bearing mice (red, n=3) or tumor-bearing mice (blue, n=4).

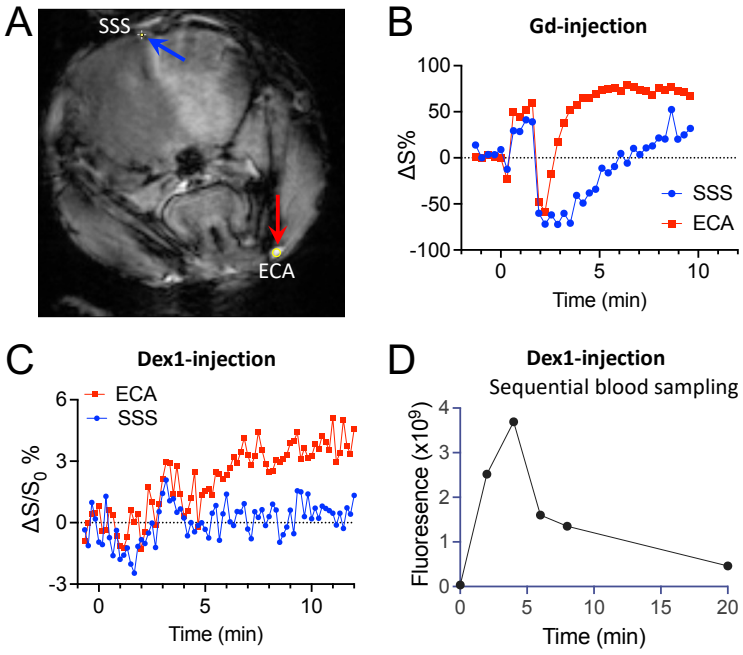

Figure S8. A) T2w image showing the locations of ROIs in the superior sagittal sinus (SSS, blue arrow) and an external carotid artery (ECA, red arrow) used to assess AIF and VOF. B) Dynamic MRI signal changes in the SSS and ECA ROIs in the Gd-CE MRI study. C) Dynamic MRI signal changes in the same SSS and ECA ROIs in the Dex1-CEST CE MRI study. D) Fluorescence intensities of blood samples drawn at different time points in a mouse receiving 10 nmol fluorescent Dex1-Cy5.5. Method: Under anesthesia, a Balb/c mouse was inserted with a 10-cm catheter (flushed with 600 unit/mL heparin solution) into the tail vein. Prior to Dex1-Cy5.5 injection, ten μL blood sample was drawn to measure the background signal of the blood. Following the injection of 10 nmol Dex1-Cy5.5 (200 μL in PBS), ten μL blood samples were drawn via the catheter at 2, 4, 6, 8, and 20 min after Dex1-Cy5.5 injection and immediately mixed with 50 uL 600 unit/mL heparin solutions. The fluorescence intensities of blood samples were measured using a Caliper IVIS Spectrum (Caliper Life Sciences, Hopkinton, MA, USA) and quantified the Live Image™ software (Caliper Life Sciences).

Reference:

1. Zhang J, Li Y, Slania S, Yadav NN, Liu J, Wang R, Zhang J, Pomper MG, van Zijl PC, Yang X, Liu G. Phenols as Diamagnetic T2 -Exchange Magnetic Resonance Imaging Contrast Agents. Chemistry 2018;24(6):1259-1263.
2. Zhang J, Han Z, Lu J, Li Y, Liao X, van Zijl PC, Yang X, Liu G. Triazoles as T2 -Exchange Magnetic Resonance Imaging Contrast Agents for the Detection of Nitrilase Activity. Chemistry 2018;24(56):15013-15018.
3. Yadav NN, Xu J, Bar-Shir A, Qin Q, Chan KW, Grgac K, Li W, McMahon MT, van Zijl PC. Natural D-glucose as a biodegradable MRI relaxation agent. Magn Reson Med 2014;72(3):823-828.
4. Swift TJ, Connick RE. NMR‐Relaxation Mechanisms of O17 in Aqueous Solutions of Paramagnetic Cations and the Lifetime of Water Molecules in the First Coordination Sphere. The Journal of Chemical Physics 1962;37(2):307-320.
5. Leigh J. Relaxation times in systems with chemical exchange: some exact solutions. Journal of Magnetic Resonance (1969) 1971;4(3):308-311.

6. Sabadini E, do Carmo Egidio F, Fujiwara FY, Cosgrove T. Use of water spin-spin relaxation rate to probe the solvation of cyclodextrins in aqueous solutions. J Phys Chem B 2008;112(11):3328-3332.